UNIVERSITY of CALIFORNIA
SANTA CRUZ

THERMAL EVOLUTION OF URANUS AND NEPTUNE WITH CONDENSATION-INHIBITED CONVECTION

A thesis submitted in partial satisfaction of the
requirements for the degree of

BACHELOR OF SCIENCE

in

ASTROPHYSICS

by

Robert Schroder

November 2020

Abstract

Thermal Evolution of Uranus and Neptune with Condensation-inhibited Convection

by

Robert Schroder

This will be the last section written, once we have finished our results and conclusion.

Contents

List of Figures

List of Tables

To Who,

M ention to who, if anyone, here

Acknowledgements

I'd like to thank....

1

Introduction

During the mid twentieth century, Frank Low observed that Jupiter was radiating away more energy than it received from the Sun (Hubbard, 1967),(Low, 1966). Shortly after this observation, theoretical work began on investigating the physics of the interior structure of the solar system gas and ice giants (Hubbard, 1977b), (Hubbard, 1977a), (M. Podolak, 1991).

At the present time, most of the giant planets in our solar system: Saturn, Jupiter, and Neptune, all have effective temperatures greater than their equilibrium temperature. Uranus is the exception. Observations of Uranus show a planet that appears to be in thermal equilibrium with its parent star, a planet with no intrinsic temperature, cooler than its more distant neighbor, Neptune, a planet of similar mass and composition. Thermal evolution models for Uranus have not matched observation, instead predicting a warmer effective temperature at 4.6 Gyr, the current age of the solar system.(Fortney et al., 2011), (M. Podolak, 1991), (W.B. Hubbard, 1995), (L. Scheibe, 2019) [There are other papers by Nettelmann 2013, Linder 2019 that I haven't looked at yet].

There have been various attempts to explain Uranus' cool temperature. Early investigations posited that a stratified interior(s), stable against convection, would allow heat to be trapped deep within the the interior (M. Podolak, 1991). Later work built on this idea, investigating the formation of stable condensation zones(Friedson & Gonzales, 2017), (Leconte et al., 2017), and (Guillot, 1995), and thermal boundary layers(N. Nettelmann, 2016), that would inhibit convection. It was speculated that the presence of these thermal boundary layers, or condensation zones, could trap heat deep within the interior, allowing the envelope above to cool more rapidly, thereby lowering the planet's effective temperature.

1.1 Condensation in Hydrogen Dominated Atmospheres

On Earth, moist air is lighter than dry air. For example, water vapor, the primary condensate in Earth's atmosphere is lighter (not by much) than the background air which is composed primarily of N_2. Thus, when H_2O condenses out of the atmosphere, there is small vertical gradient in mean molecular weight. This small gradient does not impose a significant barrier to convection. In hydrogen dominated atmospheres such as Neptune and Uarnus, the background gas is now much lighter than the condensate. When H_2O condenses out of the atmosphere a stong vertical gradient in mean molecular weaight can be established, resulting in a negative bouyancy for the parcel of gas, and hence creataing a situation where the zone is stable against convection(Guillot, 1995), (Friedson & Gonzales, 2017), (Leconte et al., 2017).

In this paper, we investigate where and when, assuming a variety deep water concentrations, whether such stable water condensation zones could form within in the outer envelope, and present their potential impact on the thermal evolution of the these planets. We decsribe our model in Chapter 2. We present our results in Chapter 3. And, we discuss our results in Chapter 4.

2

Model

2.1 Three-layer Model with Dry Adiabat

We begin with a description of the physics of our baseline structure model, starting with the conservation of mass:

$$\frac{dm}{dr} = 4\pi r^2 \rho \tag{2.1}$$

where dm is the mass contained within a sphere of radius r, and $\rho(r)$ is the density at radius r. Hydrostatic equilibrium is also assumed and described by:

$$\frac{dP}{dr} = -\frac{Gm\rho}{r^2} \tag{2.2}$$

where P is the pressure and G is the gravitational constant.

We employ a three-layer interior structure, seen schematically in Figure 2.1. At the center of the planet is a core made of rock and ice. Moving outward, the inner envelope is H_2O dominated, with uniform concentrations of H, He, and H_2O. We use the MAZEVET equation of state (EOS) (S. Mazevet & Potekhin, 2019) to define the structure of the inner envelope. The outer envelope, below 10 bars, contains trace amounts of H_2O, but is mostly H and He, dominated, and utilizes the MH13SCVH EOS (Y. Miguel & Fayon, 2018).

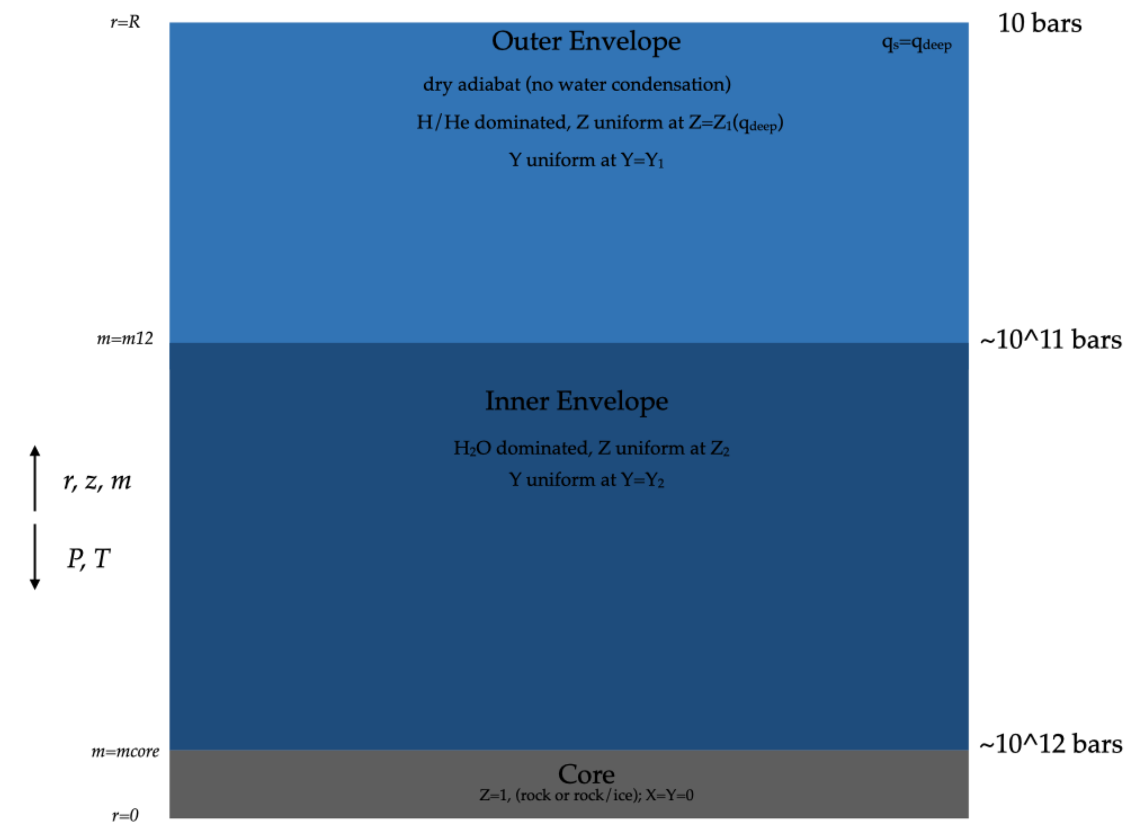

Figure 2.1: The structure for a fully convective, dry adiabatic interior. In this model, the inner and outer envelopes are assumed to be well mixed, fully convective, and following a dry adiabat. The core is composed of rock and ice. The inner envelope is water dominated, with with uniform concentrations of hydrogen, helium, and water; whereas, the outer envelope is hydrogen and helium dominated, with trace amounts of water. The 'atmosphere' exists above 10 bars.

Historically, interior structure models have assumed that the interiors are composed of compressible gasses that are statically unstable and fully convective. In a dry-convective model such as this, a parcel of gas rises as its temperature increases while its pressure remains constant. This process happens without the addition or loss of heat from the parcel, a process referred to as adiabatic. Furthermore, while there may be a critical concentration for a condensible species, this dry model does not allow for condensation. The temperature-pressure profile follows a dry adiabat gradient(R. Kippenhahn, 2012), given by:

$$\nabla_{\mathrm{ad}} = \left(\frac{\partial \ln T}{\partial \ln P}\right)_{\mathrm{s}} \tag{2.3}$$

Finally, beyond the outer envelope is the atmosphere. When modeling the thermal evolution of gas and ice giants, it has long been recognized that model atmospheres constitute an outer boundary condition for interior structure models, providing key inputs that impact cooling times for interior structure models. Our work considers both (Harold C. Graboske & Olness, 1975) and (Fortney et al., 2011) model atmospheres. Unless otherwise stated, our results will utilize the Fortney 2011 model atmospheres.

2.2 Inclusion of Moist Adiabat Within Outer Envelope

Our interior structure model modifies the baseline structure described above by adding a moist adiabatic layer to the outer envelope that, under favorable conditions, allows for the condensation of H_2O. We define the moist adiabat as follows:

$$\nabla_{\mathrm{moist}} = (1 + \frac{\frac{x_{\mathrm{vap}} L}{R_{\mathrm{gas}} T}}{\nabla_{ad} + \frac{L^2}{R_{\mathrm{gas}}^2 T^2}}) \tag{2.4}$$

where,

$$\frac{dT}{dP} = \frac{T}{P} \nabla_{\mathrm{moist}} \tag{2.5}$$

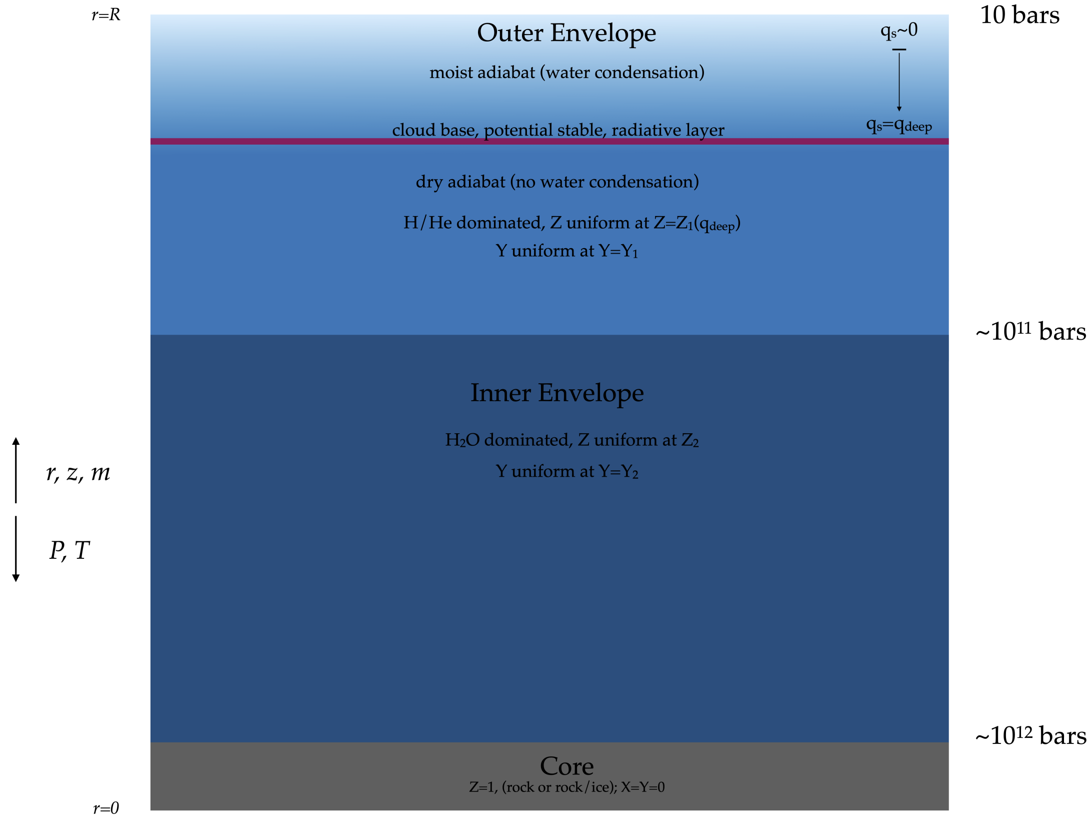

Figure 2.2: The structure for moist adiabatic interior, allowing for condensation-inhibited convection.

and the gradient of the water vapor mole fraction is given by,

$$\frac{dx_{\text{vap}}}{dP} = \frac{x_{\text{vap}}L}{R_{\text{gas}}T^2}\frac{dT}{dP} - \frac{x_{\text{vap}}}{P} \tag{2.6}$$

Gases condense at at sufficiently low temperatures or high pressures. Condensation of a gas is characterized by its saturation vapor pressure (Lavega, 2011), P_{sat}, given by:

$$P_{\text{sat}}(T) = P_{\text{sat}}(T_0)e^{-\frac{L+C_{\text{p}}T_0}{R_{\text{gas}}}(\frac{1}{T}-\frac{1}{T_0})-\frac{C_{\text{p}}}{R_{\text{gas}}}\ln\frac{T}{T_0}} \tag{2.7}$$

where $T_0 = 273.16K$.

where R_{gas} is the gas constant for the condensible species. When the partial pressure of a gas, P_{gas}, is less than P_{sat}, the parcel of gas is 'unsaturated'. When $P_{\mathrm{gas}} = P_{\mathrm{sat}}$, the gas is 'saturated'. And, when $P_{\mathrm{gas}} > P_{\mathrm{sat}}$, the parcel is 'supersaturated'. Each condensible species has its own saturation vapor pressure.

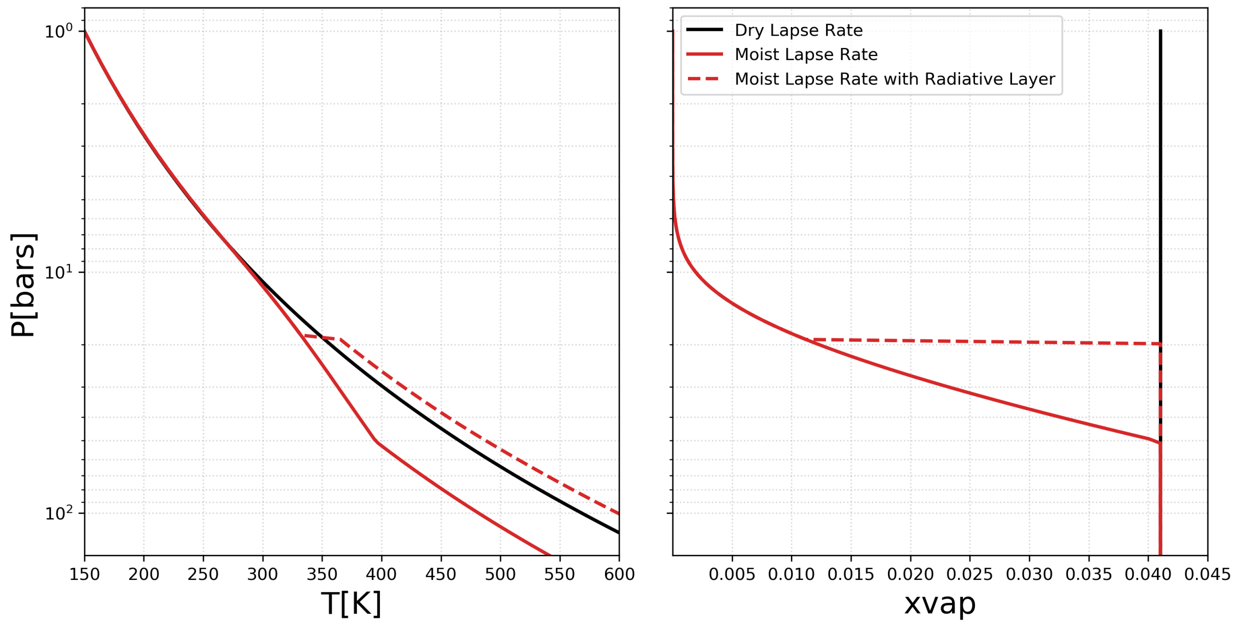

Figure 2.3: Moist vs. Dry lapse rate at t1 =

If condensation occurs, we assume that it may be stable against convection if a fast rainout occurs such that the vertical gradient in mean molecular weight is large enough to counteract the positive bouyancy of the parcel of gas (Leconte et al., 2017) (Friedson & Gonzales, 2017). In this scenario, condensation-inhibited convection occurs when α is negative, where is α (Friedson & Gonzales, 2017) is given by:

$$\alpha = 1 + \xi(q_s L/R_W T_0) \tag{2.8}$$

where R_{vap} is the gas constant for the vapor (water), T_0 is the local temperature, L is the latent heat of vaporization for water, q_s is the saturation specific humidity, and ξ is given by $\xi = \frac{1}{\epsilon} - 1$, where ϵ is the ratio of the molecular weight of vapor to the mean molecular weight of dry atmosphere. When α is negative, the vertical gradient in molecular weight results in a stabilizing effect, overwhelming the effects due to latent heat release.

2.3 Temperature Jump Across the Water Condensation Zone

Our model treats the radiative layer as a discontinuous increase in temperature. This, stable, radiative layer has a temperature profile that is governed by:

$$T(P) = T_{\text{top}} + \int_{P_{\text{top}}}^{P_{\text{base}}} \left(\frac{dT}{dP}\right)_{\text{rad}} dP \tag{2.9}$$

with P_{top} and T_{top} denote the pressure and temperature at the top of the stable water condensation(radiative) zone, and P_{base} represents the bottom of the zone. The integrand is the radiative temprature gradient (Leconte et al., 2017), defined as:

$$\left(\frac{dT}{dP}\right)_{\text{rad}} = \frac{T}{P}\nabla_{\text{rad}} = \frac{T}{P} \times \frac{3}{16}\frac{\kappa_R P}{g}\frac{T_{\text{int}}^4}{T^4} \tag{2.10}$$

The radiative temperature gradient across the layer is nearly constant, so that the integral above simplifies to:

$$T_{\text{base}} \equiv T(P + \Delta P) = T_{\text{top}} + \left(\frac{dT}{dP}\right)_{\text{rad}} \Delta P \tag{2.11}$$

where ΔP is the extent of the pressure-space of the radiative layer, given by:

$$\Delta P \equiv P_{\text{base}} - P_{\text{top}} = \frac{P_{\text{sat}}(T_{\text{base}})}{x_{\text{vap}}^{\text{deep}}} - P_{\text{top}}. \tag{2.12}$$

$$x_{\text{vap}}^{\text{sat}}(P_{\text{base}}, T_{\text{base}}) = \frac{P_{\text{sat}}(T_{\text{base}})}{P_{\text{base}}} = x_{\text{vap}}^{\text{deep}} \tag{2.13}$$

Within the condensation zone, the vapor mole fraction, x_{vap} is equal to the saturated vapor mole fraction:

$$x_{\text{vap}}(P,T) = x_{\text{vap}}^{\text{sat}}(P,T) = \frac{P_{\text{sat}}(T)}{P}, \qquad P < P_{\text{base}}. \tag{2.14}$$

The pressure and temperature at the base of the condensation zone is set by the condition that x_{vap} has reached the deep value $x_{\text{vap}}^{\text{deep}}$.

Below the condensation zone, the region is subsaturated and hence no condensation occurs. Deeper temperatures are then obtained by integrating the dry adiabat ∇_{ad}:

$$T(P > P_{\text{base}}) = T_{\text{base}} + \int_{P_{\text{base}}}^{P} \left(\frac{dT}{dP}\right)_{\text{ad}} dP \tag{2.15}$$

2.4 Energy Conservation and Thermal Evolution of Model

We borrow from conservation of energy and stellar structure and evolution to determine the timestep needed to evolve our model (R. Kippenhahn, 2012). We begin with the planets' intrinsic luminosity, defined as:

$$L_{\text{int}} = 4\pi R^2 \sigma_{\text{SB}} T_{\text{int}}^4 \tag{2.16}$$

And, the first law of thermodynamics states:

$$dQ = du + Pdv \tag{2.17}$$

where dQ is the heat added per unit mass, u is the internal energy per unit mass, and $v = \frac{1}{\rho}$ per unit mass. So, for the heat per unit mass shell, we may write:

$$dQ = (\epsilon - \frac{dL}{dm})dt \tag{2.18}$$

Substituting our equation for the first law of thermodynamics, we arrive at:

$$\frac{\partial L}{\partial m} = \epsilon - \frac{\partial u}{\partial t} + \frac{P}{\rho^2}\frac{\partial \rho}{\partial t} \tag{2.19}$$

Here, we are not dealing with any nuclear reactions, so $\epsilon = 0$, giving us:

$$\frac{\partial L}{\partial m} = \frac{\partial u}{\partial t} + \frac{P}{\rho^2}\frac{\partial \rho}{\partial t} \tag{2.20}$$

3

Results

3.1 Condensation-inhibited Convection

We began by looking at if and when condensation-inhibited convection would occur. We ran static models for a variety of T_{10}'s, or points in Uranus' past, moving from warmer (past) temperatures to cooler (recent) temperatures. The output of these static simulations are plotted in Figure 3.1. We ran our model with three different values of q_{deep}. The goal was to determine for each deep water concentration, at what pressures and temperatures, would condensation-inhibited convection occur. We found that for $q_{\text{deep}} = 0.05$, no condensation-inhibited convection occured. In other words, α (Eqn. 2.8) was never negative. However, for larger values of q_{deep}, we found that α did take on negative values in the planet's past (see rows 2 and 3 in Figure 3.1). The shaded regions of the plots indicate the pressure-space over which α is negative. We show α with respect to pressure, vapor mole fraction, and temperature. Note: the top of the shaded region in each plot would indicate the base of the condensation zone. [not sure if i should go into the issue of the reainder of the sghaded region having no physical meaning]. Looking at these plots, for $q_{\text{deep}} = 0.15$ and $q_{\text{deep}} = 0.25$, we can see that condensation inhibited convection sets in at approximately $T_{10} = 335K$. Note: The T_{10} at which the onset of condesation occurs is of course dependent on the resolution of the simulation. As such, these plots are meant to show the likelehood of condensation-inhibited convection rather than the exact moment or specific deep water concentration for which it occurs.

3.2 Formation of Radiative Zone

The plots in Figure 3.3 show the lapse rate (first column), and the change in the vapor mole fraction for H_2O (second column), for three different values of q_{deep}, 0.05, 0.15, and 0.25, for rows 1 through 3, respectively. In the first row, we can see that for early T_{10}'s, there is no onset of condensation, and the lapse rate follows a dry adiabat. For later T_{10}'s, there is a visible kink in the lapse rate which indicates the onset of condensation, at which point the lapse rate has a shallower slope. For the larger values of q_{deep}, where α takes on negative values, we see the onset of condensation-inhibited convection and the establishment of a radiative zone. In the plots, these condensation (stable, radiative)zones are represented by the horizontal discontinuites moving from left to right. As the planet cools, these radiative zones descend deeper into the planet's interior. When the radiative zones are established, the temperature jump across the radiative zone creates a warmer interior. Looking at Figure 3.2, we have overlayed the lapse rate for $q_{\text{deep}} = 0.25$ (containing radiative zones) over the lapse rate for $q_{\text{deep}} = 0.05$ (no radiative zones). From this plot, one can see that the presence of a radiative zonecreates a tempearure jump such that a given T_{10} appears to look like an earlier T_{10}. In other words, in the presence of radiative zones, the interiror appears as warm as an earlier interiror.

Looking at the adjacent x_{vap} plots, we can see that x_{vap} follows its saturated value. At the bootom of the radiative zone, the vapor mole fraction equals its deep water value, which sets the conditions for the creation of the base of the condensation zone.

3.3 Thermal Evolution of Uranus and Neptune

We simulated the thermal evolution of Uranus and Neptune with a variety of parameters. In Figure 3.4, we show the thermal evolution of Uranus, comparing the evolution of a dry adiabat, a moist adiabat with condensation but no radiative zone, and a moist adiabat with condensation with stable radiative zones. For all of these evolutionary tracks, we assumed $q_{\mathrm{deep}} = 0.25$. From these evolutionary tracks, it is clear that the coolest scenario is a moist adiabat that is never stable against convection. Interestingly, the moist adiabat that is stable against convection has the warmest outcome.

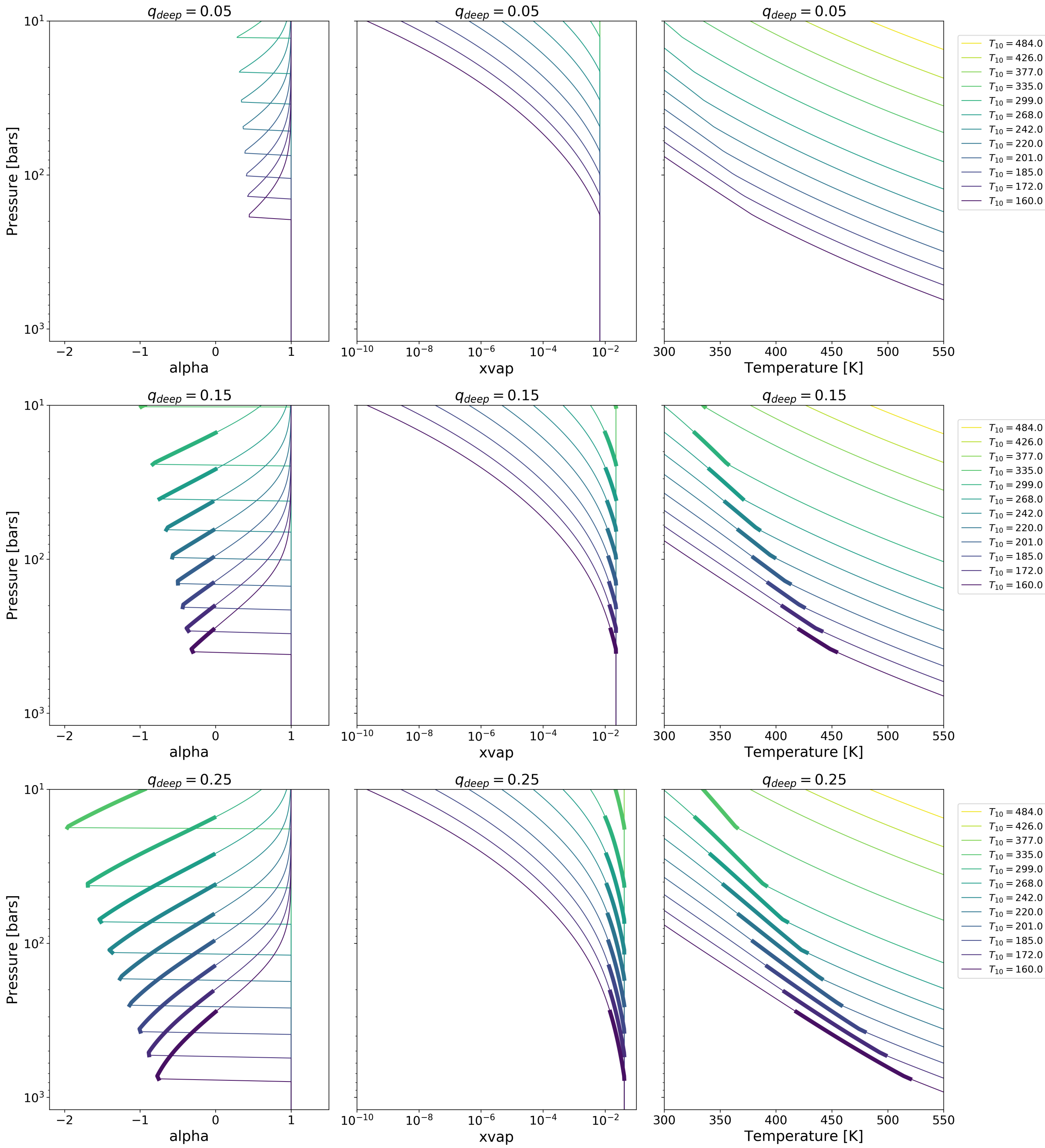

Figure 3.1: add description re: moist adiabat, when/where convection is inhibited and where the radiative zone base is in these plots. explain differences

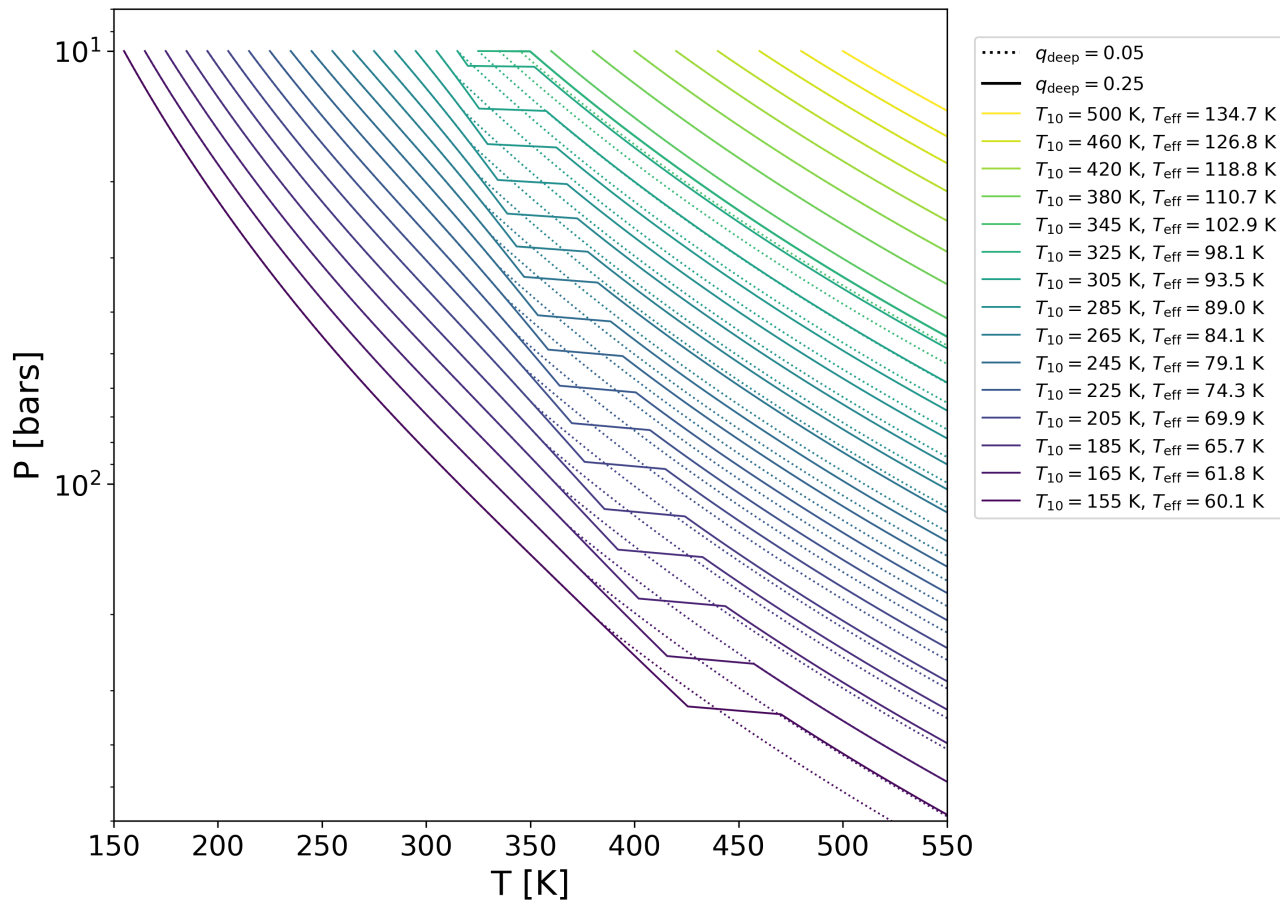

Figure 3.2: add description these plots. explain differences

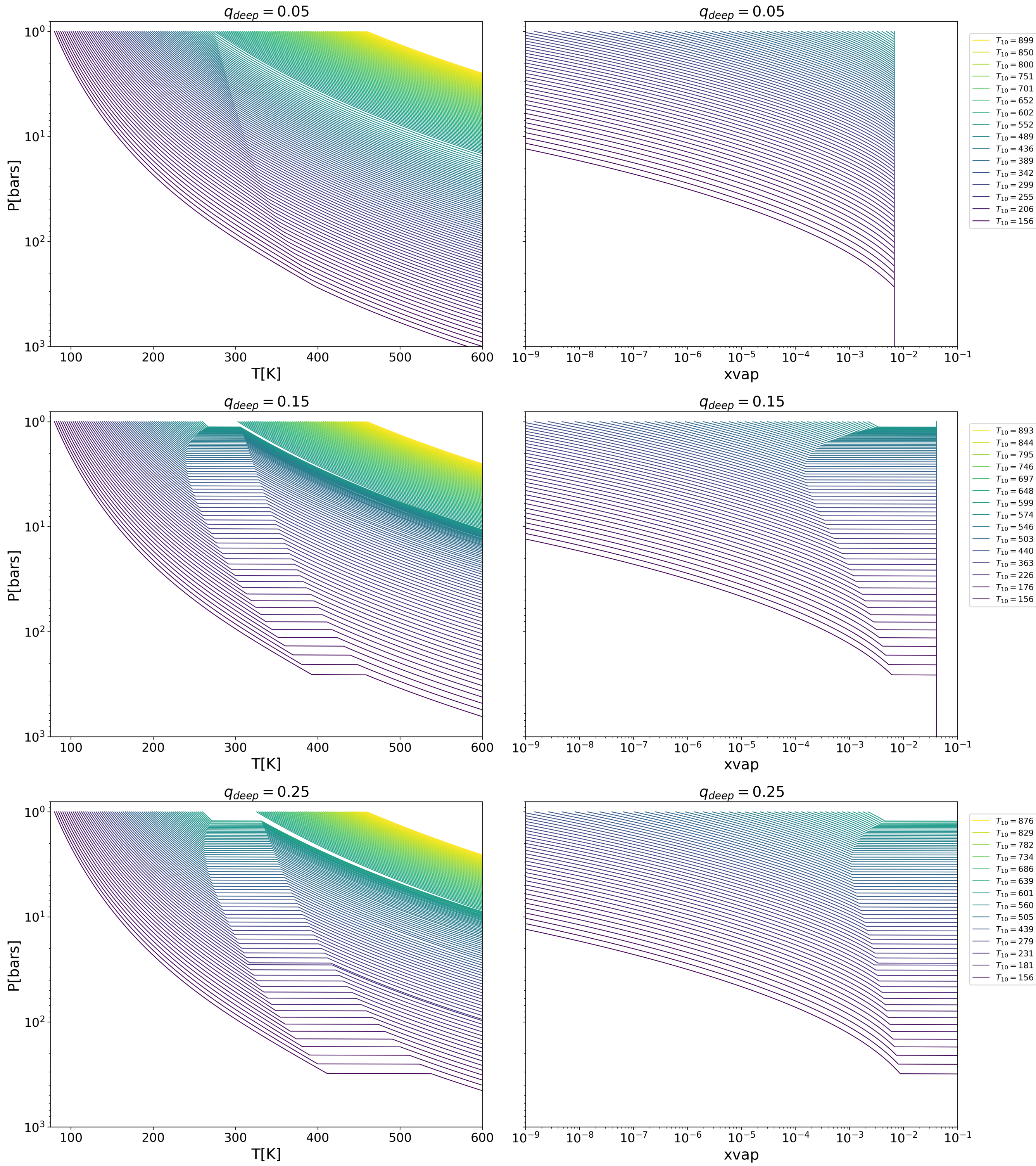

Figure 3.3: add description these plots. explain differences

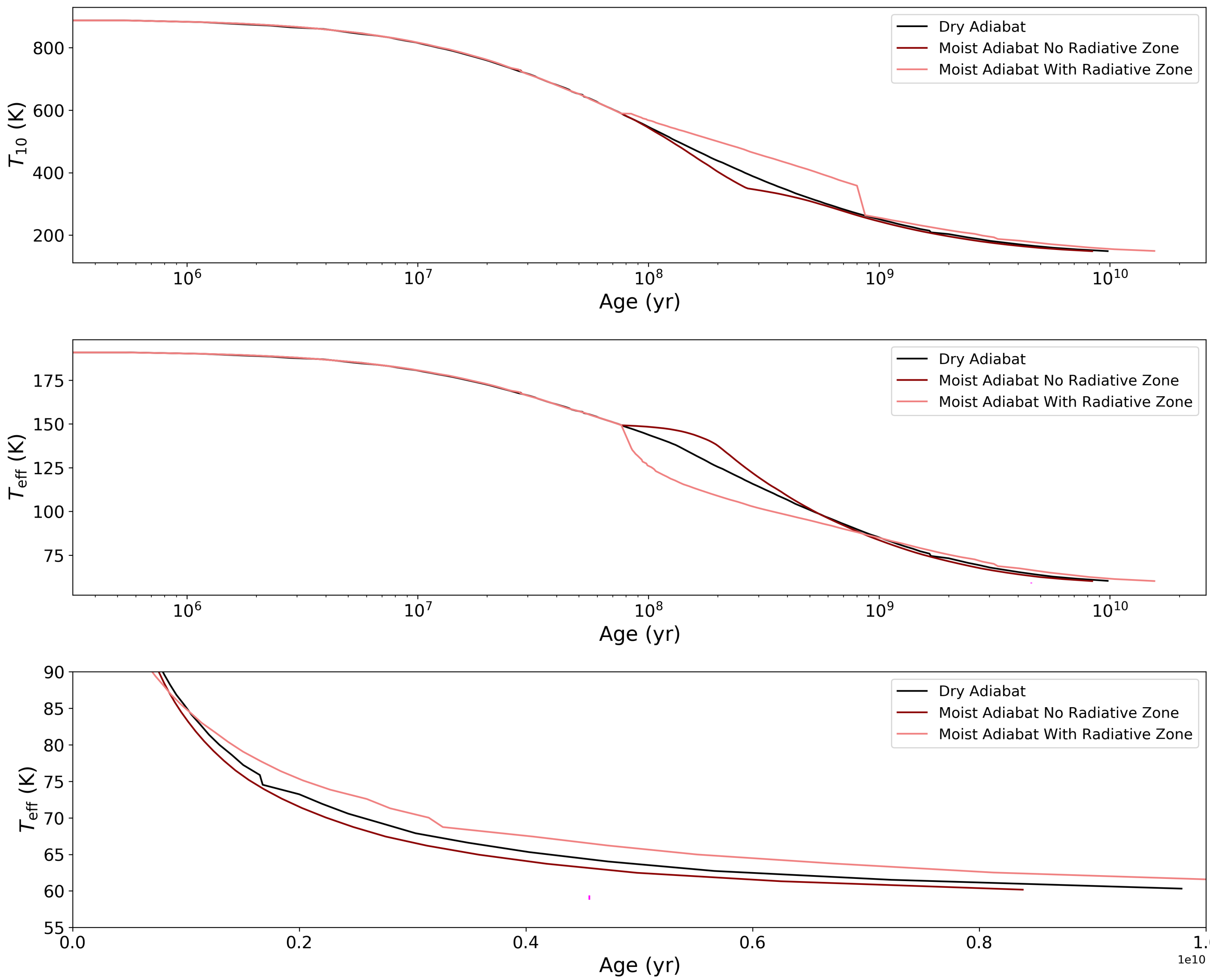

Figure 3.4: All work no play makes Jack a dull boy. All work no play makes Jack a dull boy. All work no play makes Jack a dull boy. All work no play makes Jack a dull boy. All work no play makes Jack a dull boy. All work no play makes Jack a dull boy. All work no play makes Jack a dull boy. All work no play makes Jack a dull boy. All work no play makes Jack a dull boy. All work no play makes Jack a dull boy.

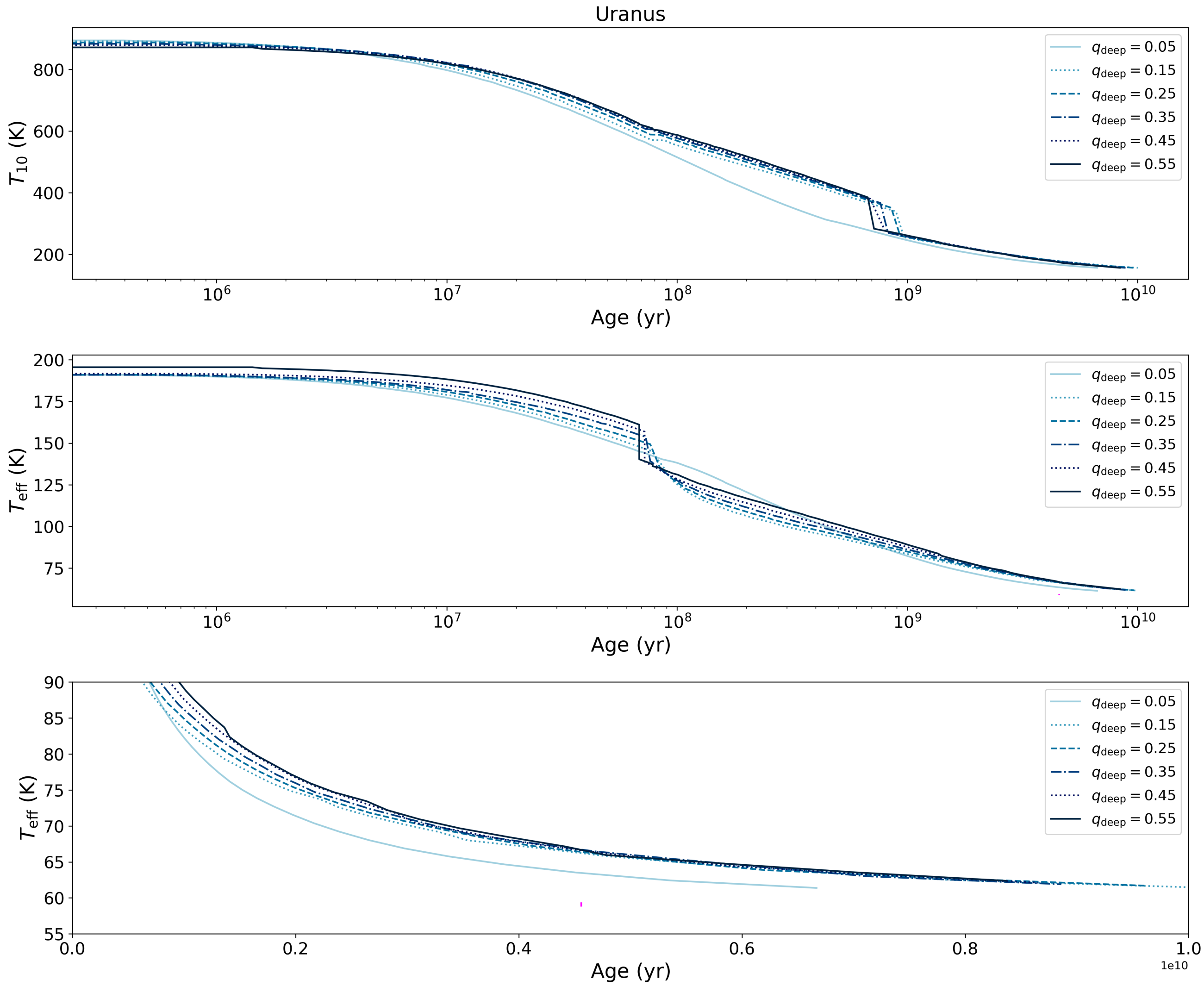

Figure 3.5: All work no play makes Jack a dull boy. All work no play makes Jack a dull boy. All work no play makes Jack a dull boy. All work no play makes Jack a dull boy. All work no play makes Jack a dull boy. All work no play makes Jack a dull boy. All work no play makes Jack a dull boy. All work no play makes Jack a dull boy. All work no play makes Jack a dull boy. All work no play makes Jack a dull boy.

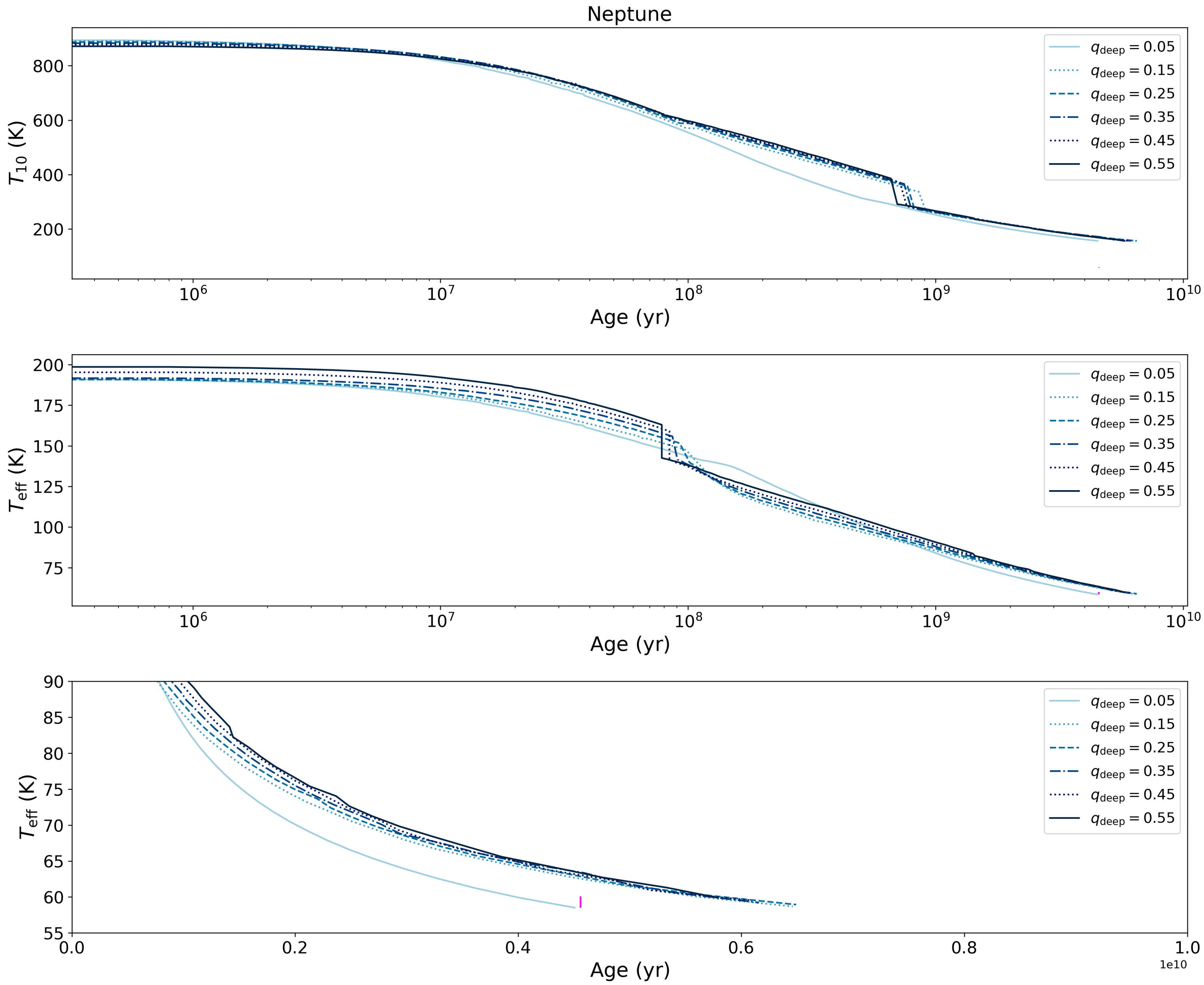

Figure 3.6: All work no play makes Jack a dull boy. All work no play makes Jack a dull boy. All work no play makes Jack a dull boy. All work no play makes Jack a dull boy. All work no play makes Jack a dull boy. All work no play makes Jack a dull boy. All work no play makes Jack a dull boy. All work no play makes Jack a dull boy. All work no play makes Jack a dull boy. All work no play makes Jack a dull boy.

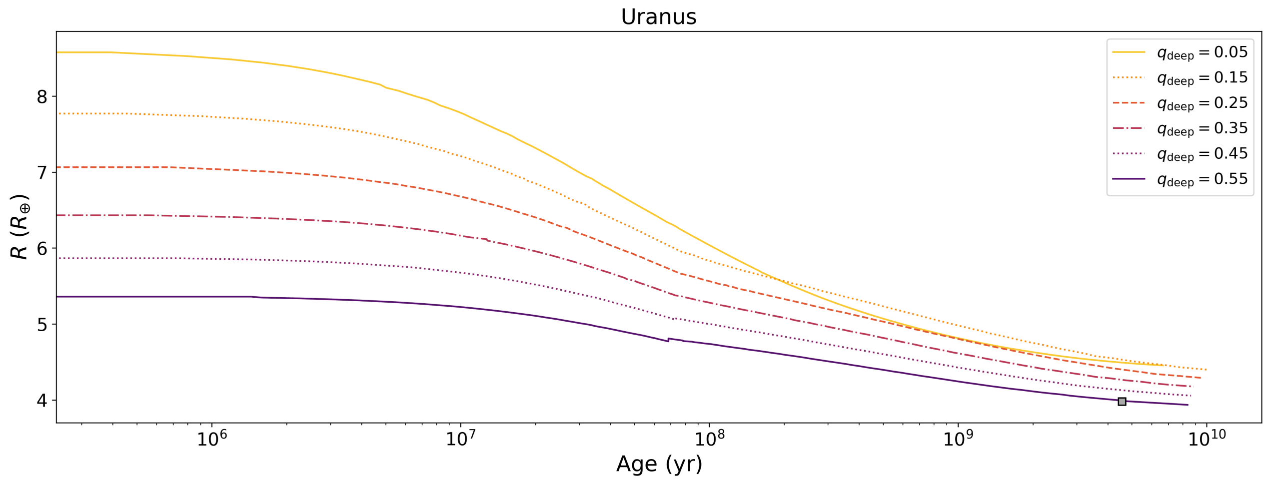

Figure 3.7: All work no play makes Jack a dull boy. All work no play makes Jack a dull boy. All work no play makes Jack a dull boy. All work no play makes Jack a dull boy.

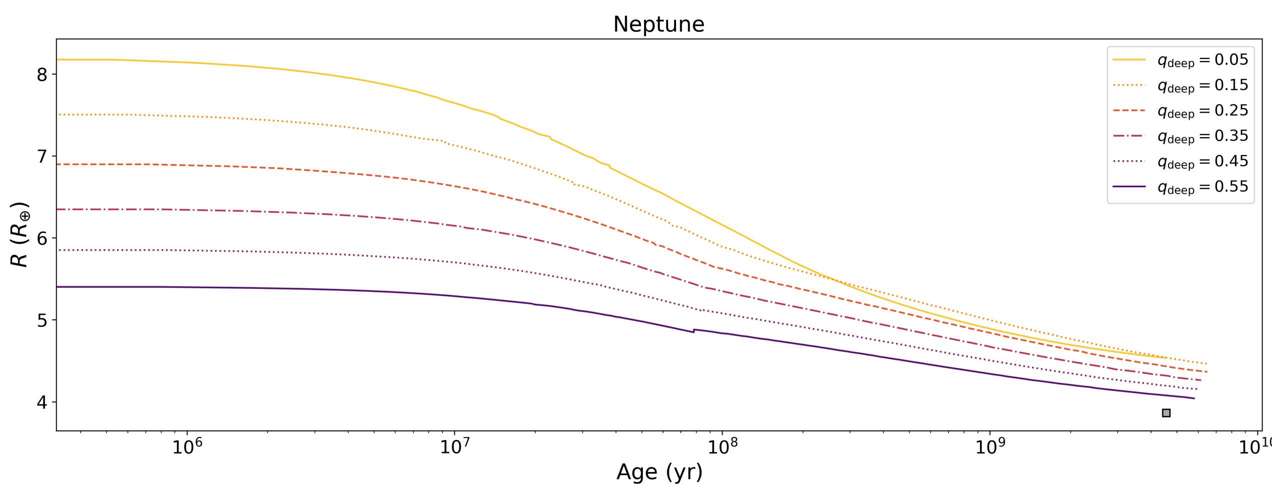

Figure 3.8: All work no play makes Jack a dull boy. All work no play makes Jack a dull boy. All work no play makes Jack a dull boy. All work no play makes Jack a dull boy.

4

Discussion and Conclusions

All work no play makes Jack a dull boy. All work no play makes Jack a dull boy.

Appendix A

Some Ancillary Stuff

Bibliography

Fortney, J. J., Ikoma, M., Nettelmann, N., Guillot, T., & Marley, M. S. (2011). Self-consistent model atmospheres and the cooling of the solar system's giant planets. *The Astrophysical Journal*, 729, 32.

Friedson, A. J. & Gonzales, E. J. (2017). Inhibition of ordinary and diffusive convection in the water condensation zone of the ice giants and implications for their thermal evolution. *Icarus*, 297, 160–178.

Guillot, T. (1995). Condensation of methane, ammonia, and water and the inhibition of convection in giant planets. *Science*, (pp. 1697–1699).

Harold C. Graboske, Jr., J. B. P. A. S. G. & Olness, R. J. (1975). The structure and evolution of jupiter: The fluid contraction. *The Astrophysical Journal*, 199, 265–281.

Hubbard, W. (1967). Thermal structure of jupiter. *The Astrophysical Journal*, 152, 745–754.

Hubbard, W. (1977a). Comparative thermal evolution of uranus and neptune. *Icarus*, , 35, 177–181.

Hubbard, W. (1977b). The jovian surface condition and cooling rate. *Icarus*, , 30, 305–310.

L. Scheibe, N Nettelmann, R. R. (2019). Thermal evolution of uranus and neptune: Adiabatic models. *Astronomy and Astrophysics*, A70, 632.

Lavega, A. S. (2011). *Introduction to Planetary Atmospheres.* Taylor and Francis Group, LLC.

Leconte, J., Selsis, F., Hersant, F., & Guillot, T. (2017). Condensation-inhibited convection in hydrogen-rich atmospheres: Stability against double-diffusive processes and thermal profiles for jupiter, saturn, uranus, and neptune. *Astronomy and Astrophysics*, A98, 598.

Low, F. (1966). Observations of venus, jupiter, and saturn at wavelength 20 microns. *Astronomical Journal*, 71, 391.

M. Podolak, W.B. Hubbard, D. S. (1991). Models of uranus' interior and magnetic field. *Uranus, Editors: J.T. Bergstralh, E.D. Miner, M. Shapely Matthews*, (pp.$\tilde{2}$9).

N. Nettelmann, K. Wangd, J. F. S. H. S. Y. M. B. R. R. (2016). Uranus evolution models with simple thermal boundary layers. *Icarus*, 275, 107–116.

R. Kippenhahn, A. Weigert, A. W. (2012). *Stellar Structure and Evolution.* Springer.

S. Mazevet, A. Licari, G. C. & Potekhin, A. Y. (2019). Ab initio based equation of state of dense water for planetary and exoplanetary modeling. *Astronomy & Astrophysics*, A128, 621.

W.B. Hubbard, D. S. (1995). The interior of neptune. *Neptune and Triton, Editor: D.P. Kruikshank*, (pp. 109).

Y. Miguel, T. G. & Fayon, L. (2018). Jupiter internal structure: the effect of different equations of state. *Astronomy & Astrophysics*, C2, 618.